Journal of Alloys and Compounds 507 (2010) 479–483

Contents lists available at ScienceDirect

Journal of Alloys and Compounds

journal homepage: www.elsevier.com/locate/jallcom

Phase structure and electrical properties of lead-free $(1-x)(Bi_{0.5}Na_{0.5})_{0.88}Ba_{0.12}TiO_3$–$xAg_{0.9}Li_{0.1}NbO_3$ piezoelectric ceramics

Lang Wu [a,*], Naiming Liu [a], Fei Zhou [a], Wenjuan Wu [b], Yuancheng Teng [a], Yuxiang Li [a]

[a] School of Material Science and Engineering, Southwest University of Science and Technology, Sichuan, Mianyang 621010, China
[b] School of Material Science and Engineering, Sichuan University, Chengdu 610064, China

ARTICLE INFO

Article history:
Received 15 June 2010
Received in revised form 21 July 2010
Accepted 27 July 2010
Available online 4 August 2010

Keywords:
Ceramics
X-ray diffraction
Ferroelectrics
Dielectric properties
Piezoelectricity

ABSTRACT

Lead-free $(1-x)(Bi_{0.5}Na_{0.5})_{0.88}Ba_{0.12}TiO_3$–$xAg_{0.9}Li_{0.1}NbO_3$ [$(1-x)$BNBT12–xALN10, x = 0–0.06] piezoelectric ceramics were synthesized by conventional oxide-mixed method. The phase structure, ferroelectric, piezoelectric, and dielectric properties of the ceramics were examined. The X-ray diffraction analysis shows that Ag^+, Li^+, and Nb^{5+} ions have diffused into the BNBT12 lattice forming a solid solution with a pure perovskite structure. The morphotropic phase boundary (MPB) between tetragonal and pseudocubic phases is formed at x = 0.01–0.02. The addition of ALN10 can improve the electrical properties of BNBT12 ceramics. The ceramics with x = 0.025 exhibit the optimum electrical properties: d_{33} = 155 pC/N, k_p = 14.8%, k_t = 40.2%, P_r = 21.9 μC/cm^2, and E_c = 2.30 kV/mm. The temperature dependence of dielectric and piezoelectric properties shows that the depolarization temperature (T_d) is shifted towards lower temperatures with increasing x. For the ceramics with $x \geq 0.03$, ferroelectric and nonpolar phases may coexist at room temperature, resulting in a sharp decline in the ferroelectricity and piezoelectricity.

1. Introduction

Perovskite Pb(Zr,Ti)O_3 (PZT) based piezoelectric ceramics have dominated the commercial market of piezoelectric devices over the past 50 years, owing to their excellent electrical properties. Recently, the demand of the sustainable development of the world and the environmental regulations has induced a new surge in developing various lead-free piezoelectric ceramics to replace the PZT-based ones [1,2].

It has shown that a large distortion of Pb in the A site of ABO_3 perovskite structure is crucial to high piezoelectric response of Pb-based materials. Fu et al. [3,4] have recently reported that the situation of Ag in $AgNbO_3$ is very similar to that of Pb in Pb-based perovskite materials. The strong covalent nature of the Ag–O bonding in $AgNbO_3$ causes a large displacement (~0.3 Å) of Ag in the perovskite structure [3]. Consequently, $AgNbO_3$ shows a large local polarization (~52 μC/cm^2) at high field (~220 kV/cm) owing to the large distortion of Ag on the A site [5]. However, pure $AgNbO_3$ exhibits very weak ferroelectricity with remnant polarization (P_r) of 0.041 μC/cm^2 at zero field, which is believed to be derived from the small displacement of Nb^{5+} in the B site [5]. It has also been reported that a partial substitution of Li for Ag can induce a ferroelectric rhombohedral distortion [3,6], which can be attributed to the Ag displacement by the large off-centering nature of Li in the perovskite structure [7]. In particular, a large P_r of 23 μC/cm^2 was observed for the $Ag_{0.9}Li_{0.1}NbO_3$ (ALN10) ceramics at room temperature [6]. Therefore, it can be expected that by incorporating Ag and Li into A site of perovskite structure, it would show high ferroelectric and piezoelectric properties owing to the large distortion of the structure.

On the other hand, morphotropic phase boundary (MPB) plays a significant role in PZT-based ceramics because the piezoelectric and dielectric properties show a maximum over a specific compositional range around the MPB. $Bi_{0.5}Na_{0.5}TiO_3$ (BNT) has a perovskite structure with a rhombohedral symmetry at room temperature, which is considered to be an excellent candidate for lead-free piezoelectric ceramics because of its large remnant polarization (P_r = 38 μC/cm^2) and high Curie temperature (T_c = 320 °C) where the permittivity has a maximum [8]. However, because of their high coercive field (E_c = 73 kV/cm), pure BNT ceramics are very difficult to polarize and their piezoelectric properties (d_{33} = 72.9 pC/N) are not desirable [9]. It has been shown that BNT can form a MPB with other perovskites, such as $BaTiO_3$ (BT) [10], $Bi_{0.5}K_{0.5}TiO_3$ (BKT) [11], and $KNbO_3$ (KN) [12], and these MPB compositions exhibit much better piezoelectric properties than pure BNT ceramics. However, the depolarization temperature (T_d) usually shifts downward from 187 °C for pure BNT to approximately 100 °C for the MPB composition [9,10–13]. According to our previous work [14], the tetragonal side of the MPB composition in the BNT–BT system possesses both relatively high depolarization temperature (T_d ~ 190 °C) and high d_{33} values. However, the piezoelectric properties of the ceramics are still unfavorable for application (d_{33} ~ 130 pC/N).

* Corresponding author. Tel.: +86 816 2419201; fax: +86 816 2419201.
E-mail address: lang.wu@163.com (L. Wu).

0925-8388/$ – see front matter © 2010 Elsevier B.V. All rights reserved.
doi:10.1016/j.jallcom.2010.07.208

Based on the above consideration, we tried to design a new solid solution between $(Bi_{0.5}Na_{0.5})_{0.88}Ba_{0.12}TiO_3$ (BNBT12) and ALN10, possessing tetragonal and rhombohedral phases, respectively. It is expected to form a MPB composition in the BNBT12–ALN10 system. It is reasonable to anticipate that the BNBT12–ALN10 solid solution would possess high piezoelectric properties due to the formation of MPB and the large distortion of Ag and Li in the A site. In this work, the phase structure, ferroelectric, and piezoelectric properties of $(1-x)$BNBT12–xALN10 lead-free piezoelectric ceramics are investigated, the relationship between the phase structure and electrical properties is also discussed.

2. Experimental

The $(1-x)$BNBT12–xALN10 ($x = 0$–0.06) ceramics were prepared by the conventional oxide-mixed method. The oxide or carbonate powders of Bi_2O_3 (99%), TiO_2 (98%), $BaCO_3$ (99%), Na_2CO_3 (99.8%), Li_2CO_3 (97%), Nb_2O_5 (99%), and Ag_2O (99%) were selected as the starting raw materials. The powders in the stoichiometric ratio of the compositions were mixed in alcohol by ball milling. Then the mixture was calcined at 950 °C for 2 h. The synthesized powders were again ball milled, granulated, and pressed into discs by dry pressuring with diameters of 13 mm and thicknesses of 1.1 mm. The compacted disks were sintered in air between 1100 and 1200 °C for 2 h. Silver slurry was coated on both sides of the discs and then treated at 700 °C for 10 min as electrodes. The specimens were polarized in silicone oil at 60 °C under 4 kV/mm for 20 min.

The bulk densities of the sintered samples were measured by Archimedes' method. The microstructures were observed using scanning electron microscopy (SEM, JSM-5900LV). X-ray diffraction (XRD) characterization of the ceramics was performed using Cu Kα radiation in the $\theta-2\theta$ scan mode (D/max-2500PC). The piezoelectric constant (d_{33}) was measured using a piezo-d_{33} meter (ZJ-3A). The electromechanical coupling factors (k_p and k_t) and the mechanical quality factor (Q_m) were measured using an impedance analyzer (HP 4294A). The dielectric constant (ε_r) and dielectric loss ($\tan\delta$) of the samples were measured using an impedance analyzer (HP 4278A). The remnant polarization (P_r) and coercive field (E_c) were determined from polarization versus electric field (P–E) hysteresis loops measured by a Radiant Precision Workstation (USA).

3. Results and discussion

Fig. 1 presents the surface images of $(1-x)$BNBT12–xALN10 ceramics with (a) $x = 0$ and (b) $x = 0.02$. It can be observed in Fig. 1 that the grain boundary is clear and almost no visible pores are found in both samples. It is also found that all ceramic samples have high densities about 5.71–5.80 g/cm^3, which are more than 95% of the theoretical values. Furthermore, it can be noted that the incorporation of ALN10 into BNBT12 has no obvious effect on the grain size, which is about 2–5 μm for all samples.

Fig. 2 shows the XRD patterns of $(1-x)$BNBT12–xALN10 ceramics. It can be determined from Fig. 2(a) that all of the samples have a pure perovskite structure. ALN10 appears to have diffused into the BNBT12 lattice forming a solid solution. According to the principles of crystal chemistry, Ag^+ (1.15 Å) and Li^+ (0.76 Å) ions most likely occupy the Na^+ (1.02 Å) sites of $(1-x)$BNBT12–xALN10 ceramics, while Nb^{5+} (0.64 Å) ions may enter the B sites for substituting Ti^{4+} (0.605 Å) ions [15]. Similar to PZT-based ceramics, the Nb^{5+} can be considered as a donor-type additive in this system. The XRD patterns of the samples in the 2θ range of 44–48° are shown in Fig. 2(b). For $x < 0.01$, the crystal structures of the samples are tetragonal symmetry, which is characterized by a (0 0 2)/(2 0 0) peak splitting between 45° and 47°. The lattice anisotropy c/a of the BNBT12 ceramics is about 1.0170. The tetragonality of the $(1-x)$BNBT12–xALN10 ceramics decreases with increasing x. When $x \geq 0.02$, the lattice anisotropy is very small (~1.0006) and no peak splitting can be observed. It seems that the crystal structures of the samples transform to pseudocubic symmetry. A MPB between tetragonal and pseudocubic phases of $(1-x)$BNBT12–xALN10 ceramics may exist at $x = 0.01-0.02$. This is similar to the results reported for the BKT–KN ceramics [16]. Additional experimental data will be provided below for further discussion.

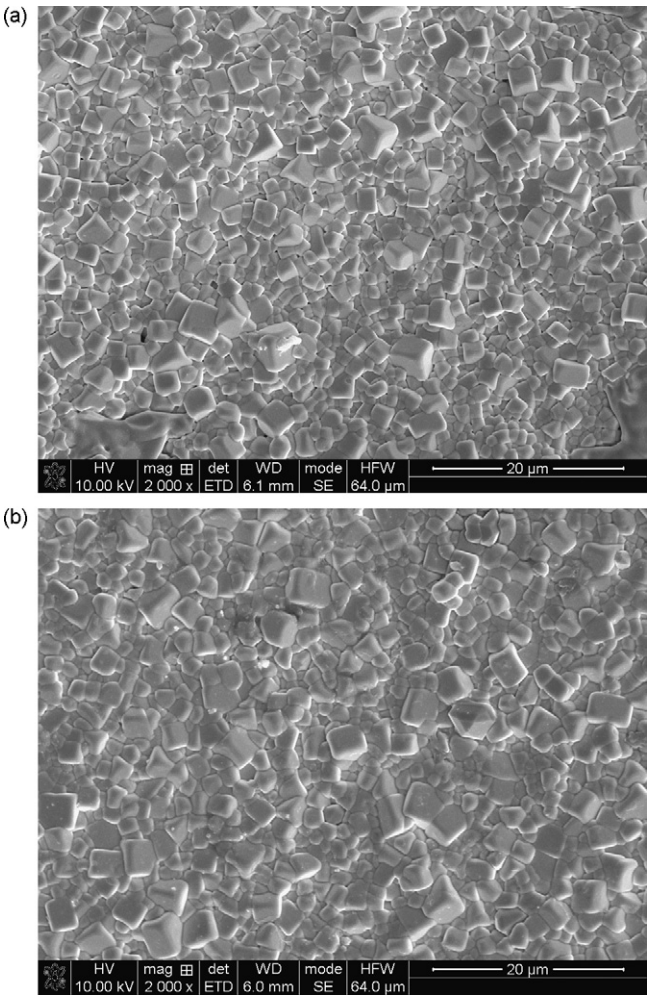

Fig. 1. SEM micrographs of $(1-x)$BNBT12–xALN10 ceramics with (a) $x = 0$ and (b) $x = 0.02$.

Fig. 3(a) shows the P–E hysteresis loops of the $(1-x)$BNBT12–xALN10 ceramics with $x = 0$, 0.02, 0.03, and 0.04. P_r and E_c of the samples as a function of x are shown in Fig. 3(b). It was found that normal P–E hysteresis loops were observed for the ceramics with $x \leq 0.025$. However, the P–E loop becomes slightly deformed at $x = 0.03$. The loop appears to form a double-like P–E hysteresis loop at $x = 0.04$ (Fig. 3(a)). It can be observed in Fig. 3(b) that the E_c decreases almost linearly with increasing x. The P_r increases slightly from 19.2 to 23.0 μC/cm^2 as x increases from 0 to 0.03. With further raise of x, the P_r decreases significantly and the ferroelectricity becomes very weak as the P–E hysteresis loop becomes "pinched". For the ceramics with $x = 0.04$, the P_r and E_c of the sample are only 6.33 μC/cm^2 and 1.18 kV/mm, respectively. Similar to $K_{0.5}Na_{0.5}NbO_3$ (KNN)-modified BNT–BT system [17], ferroelectric phase and nonpolar phase may coexist as a matastable phase in the samples with $x = 0.03$ and 0.04. The ferroelectric phase dominates in the sample with $x = 0.03$ while the nonpolar one becomes dominant at $x = 0.04$. On the other hand, these results also confirm that the crystal structures of the samples with $x = 0.02$–0.04 are not true cubic symmetry but a pseudocubic structure because the perovskite material with cubic symmetry has no spontaneous polarization.

Table 1 presents the electrical properties of $(1-x)$BNBT12–xALN10 ceramics. It can be noted in Table 1 that d_{33} increases with increasing x and reaches the maximum value of 155 pC/N at $x = 0.025$. At $x = 0.04$, the d_{33} drops to about

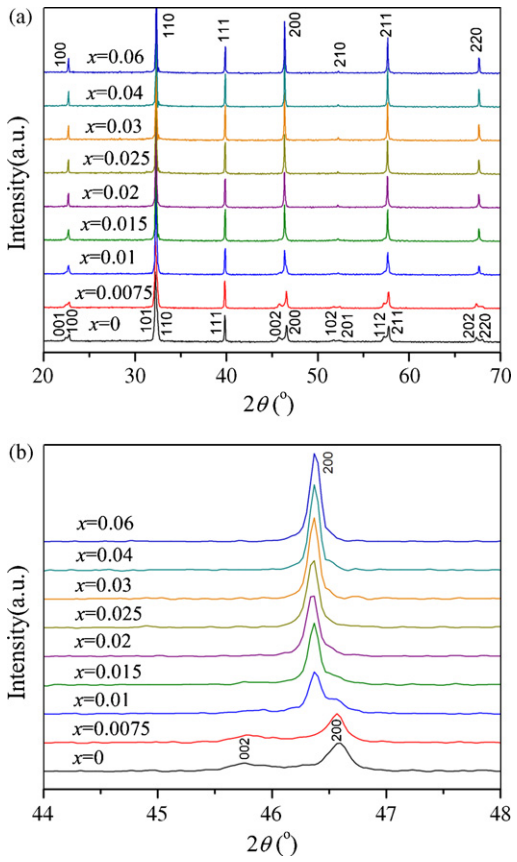

Fig. 2. XRD patterns of $(1-x)$BNBT12–xALN10 ceramics in the 2θ range: (a) 20–70° and (b) 44–48°.

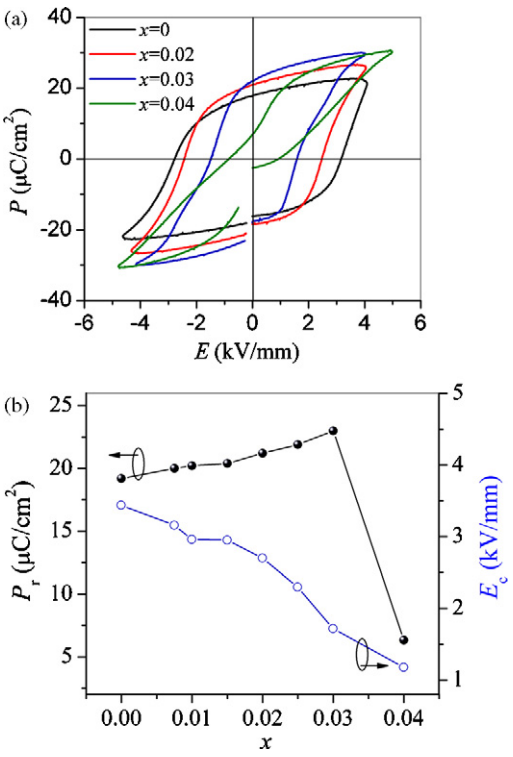

Fig. 3. (a) P–E hysteresis loops of the $(1-x)$BNBT12–xALN10 ceramics with $x=0$, 0.02, 0.03, and 0.04; (b) P_r and E_c of the samples as a function of x.

9 pC/N. In addition, k_p and k_t increase slightly with increasing x. The maximum values of k_p (14.8%) and k_t (45.1%) are observed at $x=0.025$ and 0.01, respectively. Dielectric constant ε_r of the ceramics before (ε_1) and after (ε_2) poling increase with increasing x, as shown in Table 1. The increase in ε_r may be attributed to the presence of donor cations (Nb^{5+}) in the lattices. The Q_m of the ceramics decreases with increasing x. These results indicate that the ceramics with $x=0.025$ possess the optimum piezoelectric properties: $d_{33}=155$ pC/N, $k_p=14.8\%$, $k_t=40.2\%$.

As mentioned above, the addition of ALN10 decreases the tetragonality of BNBT12 ceramics. The E_c of the $(1-x)$BNBT12–xALN10 ceramics decreases with increasing x. The lower E_c values can make the ceramics polarize sufficiently in poling process, which is very helpful to the increase in piezoelectric properties. Additionally, for the compositions near tetragonal-pseudocubic MPB in this system, the improvement of symmetry can reduce the internal stress of the domain reorientation and make the domains transform more easily in the poling process, which can also increase the piezoelectric properties [12,18]. On the other hand, according to thermodynamic theory of ferroelectrics [19], piezoelectric properties are proportional to the polarization and the dielectric constant. For the ceramics with $x>0.03$, though the ε_r value is relatively high (~1530), the P_r is too small (~6.33 μC/cm²) that the piezoelectricity almost disappears. In this study, we expect that the strong hybridization between Ag and O atoms and the large off-centering nature of Li can improve the ferroelectric and piezoelectric properties of BNBT12 ceramics. However, the nonpolar phases become dominant and the T_d is shifted towards below room temperature when $x>0.03$, resulting in the sharp decline of the piezoelectric properties. Therefore, the amount of Ag and Li additive has been limited. The effect of the structural distortion caused by Ag and Li on the ferroelectric and piezoelectric properties might not be so significant, owing to their low concentration level in this system.

Fig. 4(a)–(e) shows the temperature dependence of ε_r and tan δ of poled $(1-x)$BNBT12–xALN10 ceramics with $x=0$, 0.01, 0.02, 0.03, and 0.04, respectively, at different frequencies ranging from

Table 1
Electrical properties of $(1-x)$BNBT12–xALN10 ceramics. ε_1 and ε_2 are dielectric constant before and after poling, respectively.

Samples	$x=0$	$x=0.01$	$x=0.015$	$x=0.02$	$x=0.025$	$x=0.03$	$x=0.04$
Density ρ (g/cm³)	5.75	5.71	5.72	5.73	5.72	5.73	5.74
d_{33} (pC/N)	126	140	143	150	155	152	9
k_p (%)	13.7	14.1	14.3	14.6	14.8	13.2	–
k_t (%)	41.2	45.1	44.6	44.1	40.2	36.9	–
Q_m	106	101	98	90	77	72	–
ε_1 (1 kHz)	705	1100	1240	1370	1400	1430	1440
ε_2 (1 kHz)	775	872	888	1010	1150	1350	1530
tan δ (1 kHz)	0.029	0.031	0.036	0.036	0.041	0.050	0.061
P_r (μC/cm²)	19.2	20.2	20.4	21.2	21.9	23.0	6.33
E_c (kV/mm)	3.44	2.96	2.95	2.70	2.30	1.72	1.18
T_d (°C)	195	150	140	130	120	92	–
T_m (°C)	272	265	250	245	243	242	232

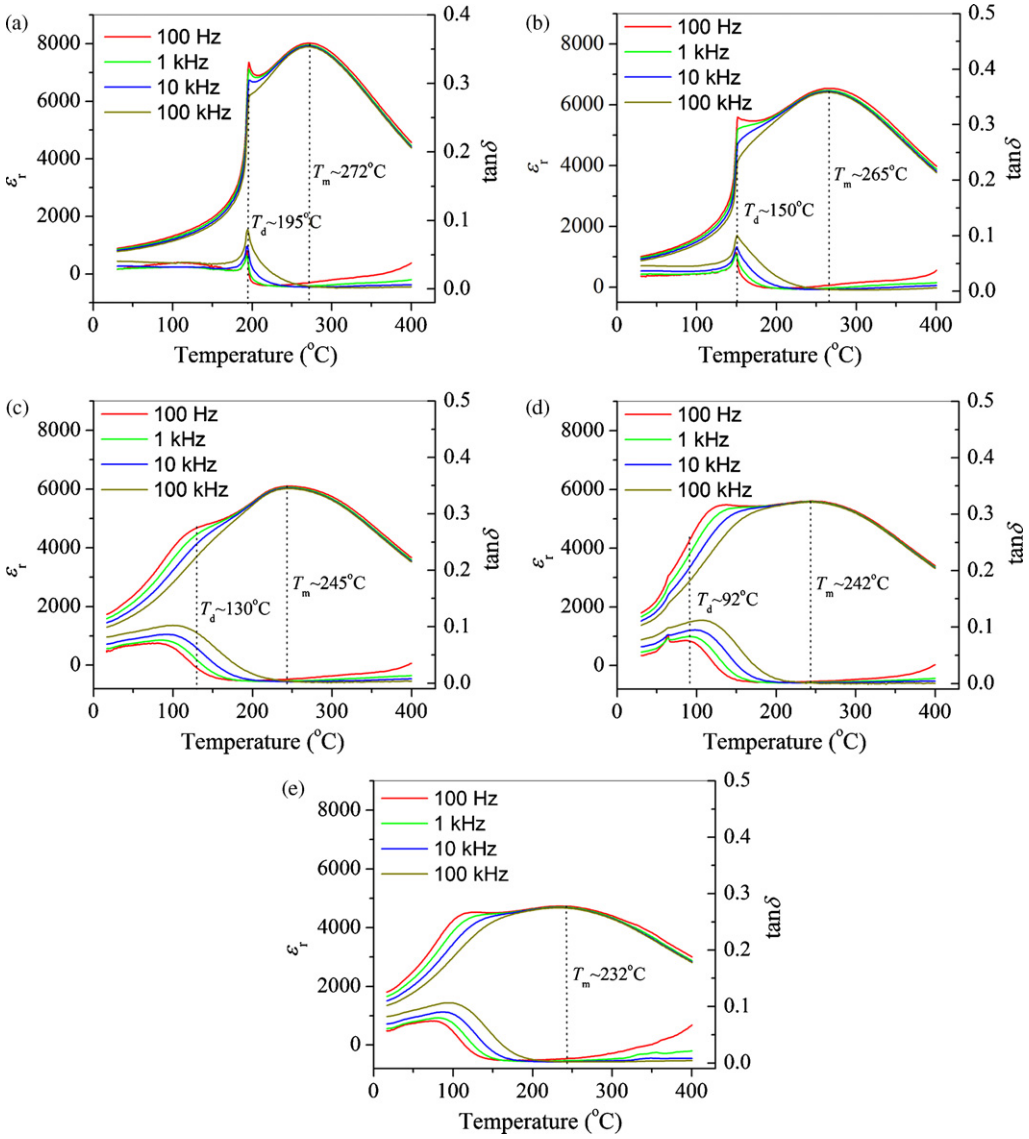

Fig. 4. Temperature dependence of ε_r and tan δ of poled $(1-x)$BNBT12–xALN10 ceramics at different frequencies ranging from 100 Hz to 100 kHz: (a) $x = 0$; (b) $x = 0.01$; (c) $x = 0.02$; (d) $x = 0.03$; and (e) $x = 0.04$.

100 Hz to 100 kHz. For BNBT12 ceramics (i.e., $x = 0$), a sharp increase in the ε_r and tan δ near 195 °C is observed, which corresponds to the T_d. At temperatures higher than T_d, the ε_r increases gradually with increasing temperature and reaches the maximum value at a temperature T_m (~272 °C). In addition, after an abrupt jump in the ε_r versus temperature curves, a relaxor-like behavior can be observed near T_d (Fig. 4(a)). This indicates that a transformation between a normal and a relaxor-ferroelectric state occurs near T_d, which is very similar to the results obtained for $(Bi_{0.5}Na_{0.5})_{0.70}Ba_{0.30}TiO_3$ ceramics [20]. It can also be noted in Fig. 4 that the maximum values of ε_r decline with increasing x and the ε_r versus temperature curves become more and more flat. Furthermore, both T_d and T_m are shifted towards low temperatures with increasing x. The ceramics with $x = 0.01$ show similar dielectric response as the BNBT12 ceramics. The T_d and T_m of the sample ($x = 0.01$) are 150 and 265 °C, respectively.

A different dielectric behavior is observed for the samples with $x = 0.02$, 0.03, and 0.04 (Fig. 4(c)–(e)). Firstly, it shows a typical relaxation behavior for these samples from room temperature to about 200 °C. Namely, with increasing frequency, the values of ε_r decrease while the values of tan δ increase in this temperature range. It suggests that the pseudocubic symmetry of the samples with $x \geq 0.02$ is a relaxor-ferroelectric phase. Similar pseudocubic relaxor-ferroelectric phase has also been observed in $(1-x)$BNT $-$ xKN ($x \geq 0.08$) [13] and $(1-x)$BNT $-$ xBa$(Al_{1/2}Sb_{1/2})O_3$ system ($x \geq 0.045$) [21]. Secondly, the anomaly of tan δ exhibits obvious frequency dispersion and it does not show a sharp peak, owing to the relaxation behavior of the samples with pseudocubic structure. So it is very difficult to determine the T_d accurately from the temperature dependence of dielectric properties. In this study, the T_d of the samples with $x > 0.01$ was determined from the temperature dependences of piezoelectric properties.

Fig. 5 shows the d_{33} of the ceramics with $x = 0$, 0.01, 0.02, and 0.03 as a function of annealing temperature. It was found that d_{33} had a steep fall after the samples were treated at a certain temperature for 30 min, which is defined as the T_d in the present work. The T_d is about 130 and 92 °C for the ceramics with $x = 0.02$ and 0.03, respectively. As the ferroelectric and piezoelectric properties of the sample with $x = 0.04$ are very weak at room temperature, it is difficult to determine its T_d, which might be already below room temperature. Additionally, it should be noted that the poled $(1-x)$BNBT12–xALN10 samples also possess d_{33} val-

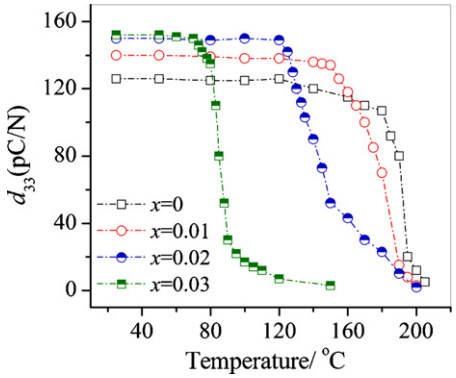

Fig. 5. d_{33} of $(1-x)$BNBT12–xALN10 ceramics with $x = 0$, 0.01, 0.02, and 0.03 as function of annealing temperature.

ues of 5–15 pC/N after they were annealed above T_d. This result also indicates that the polar and nonpolar regions may coexist at temperatures between T_d and T_m [17,21,22].

4. Conclusions

$(1-x)$BNBT12–xALN10 ($x = 0$–0.06) lead-free piezoelectric ceramics were prepared by the conventional ceramic fabrication technique. The effects of amount of ALN10 on the phase structure and electrical properties of the ceramics were studied. The XRD analysis shows that all of the samples have a single-phase perovskite structure and ALN10 appears to have diffused into the BNBT12 lattice forming a solid solution. The MPB between tetragonal ferroelectric and relaxor-ferroelectric pseudocubic phases of $(1-x)$BNBT12–xALN10 ceramics is formed at approximately $x = 0.01$–0.02. The addition of ALN10 can improve the piezoelectric, ferroelectric, and dielectric properties of BNBT12 ceramics. The ceramics with $x = 0.025$ exhibit the optimum electrical properties: $d_{33} = 155$ pC/N, $k_p = 14.8\%$, $k_t = 40.2\%$, $P_r = 21.9\ \mu C/cm^2$, and $E_c = 2.30$ kV/mm. The temperature dependence of dielectric and piezoelectric properties shows that both T_d and T_m are shifted towards low temperatures with increasing x. Ferroelectric and nonpolar phases may coexist in the samples with $x \geq 0.03$ at room temperature. This system shows favorable properties such as large ratio of k_t/k_p and high d_{33}, which are suitable for the applications in piezoelectric ultrasonic devices.

Acknowledgements

This work was supported by NSFC Projects (10775113), and the Doctorial Project of Southwest University of Science and Technology (08zx0112).

References

[1] E. Cross, Nature 432 (2004) 24–25.
[2] Y. Saito, H. Takao, T. Tani, T. Nonoyama, K. Takatori, T. Homma, T. Nagaya, M. Nakamura, Nature 432 (2004) 84–87.
[3] D. Fu, M. Endo, H. Taniguchi, T. Taniyama, S. Koshihara, M. Itoh, Appl. Phys. Lett. 92 (2008) 172905.
[4] I. Grinberg, A.M. Rappe, Appl. Phys. Lett. 85 (2004) 1760–1762.
[5] D. Fu, M. Endo, H. Taniguchi, T. Taniyama, M. Itoh, Appl. Phys. Lett. 90 (2007) 252907.
[6] Y. Sakabe, T. Takeda, Y. Ogiso, N. Wada, Jpn. J. Appl. Phys. 40 (2001) 5675–5678.
[7] D.I. Bilc, D.J. Singh, Phys. Rev. Lett. 96 (2006) 147602.
[8] G.A. Smolenskii, V.A. isupov, A.I. Agranovskaya, N.N. Krainik, Sov. Phys. Solid State 2 (1961) 2651–2654.
[9] Y. Hiruma, H. Nagata, T. Takenaka, J. Appl. Phys. 105 (2009) 084112.
[10] T. Takenaka, K. Maruyama, K. Sakata, Jpn. J. Appl. Phys. 30 (1991) 2236–2239.
[11] A. Sasaki, T. Chiba, Y. Mamiya, E. Otsuki, Jpn. J. Appl. Phys. 38 (1999) 5564–5567.
[12] G. Fan, W. Lu, X. Wang, F. Liang, J. Xiao, J. Phys. D: Appl. Phys. 41 (2008) 035403.
[13] Y. Hiruma, H. Nagata, T. Takenaka, J. Appl. Phys. 104 (2009) 124106.
[14] L. Wu, D.Q. Xiao, D.M. Lin, J.G. Zhu, P. Yu, X. Li, Jpn. J. Appl. Phys. 46 (2007) 7382–7387.
[15] R.D. Shannon, Acta Crystallogr. A 32 (1976) 751–767.
[16] T. Wada, K. Toyoike, Y. Imanaka, Jpn. J. Appl. Phys. 40 (2001) 5703–5705.
[17] W. Jo, T. Granzow, E. Aulbach, J. Rödel, D. Damjanovic, J. Appl. Phys. 105 (2009) 094102.
[18] G. Fan, W. Lu, X. Wang, F. Liang, Appl. Phys. Lett. 91 (2007) 202908.
[19] D. Damjanovic, Rep. Prog. Phys. 61 (1998) 1267–1324.
[20] J. Suchanicz, J. Kusz, H. Böhm, H. Duda, J.P. Mercurio, K. Konieczny, J. Eur. Ceram. Soc. 23 (2003) 1559–1564.
[21] Y. Hiruma, H. Nagata, T. Takenaka, Appl. Phys. Lett. 95 (2009) 052903.
[22] D.M. Lin, K.W. Kwok, H.L.W. Chan, Solid State Ionics 178 (2008) 1930–1937.